



# Dual-Energy: The Siemens Approach

Bernhard Schmidt and Thomas Flohr

## Contents

1	<b>General Aspects and Workflow</b> .....	15
2	<b>Dual Source-Based Dual-Energy</b> .....	19
3	<b>Twin Spiral Dual-Energy</b> .....	22
4	<b>TwinBeam Dual-Energy</b> .....	23
5	<b>Conclusions</b> .....	26
	<b>References</b> .....	26

## 1 General Aspects and Workflow

The first medical CT scanner capable of DE scanning by means of fast kV-switching was the SOMATOM DRH introduced by Siemens in 1987 (Kalender 1987). It allowed for dual-energy acquisitions in topogram and axial scan mode; however,

the main clinical benefit of this new technical capability was a significant improvement in the accuracy of bone mineral density quantification. Although several clinical studies demonstrated the advantage of DE CT over single energy CT especially in the presence of fat—elimination of the so-called “fat error”—(Laval-Jeantet 1986; Genant 1977; Vetter 1986), the fast kV-switching technique to acquire DE data was abandoned in subsequent CT systems. Technical limitations led to compromised scan data acquisition, degradation in image quality, and increased radiation dose to the patient since attenuation-based tube current modulation and necessary adaptations of the tube current between the kV-switches was not feasible due to basic physical limitations of the technology. On top of this new technical opportunities such as DEXA (dual-emission X-ray absorptiometry) became available and limited the need for DE CT bone densitometry. Other clinically relevant applications, however, were not within reach at that time.

---

B. Schmidt (✉)  
Siemens Healthcare GmbH, Computed Tomography,  
Forchheim, Germany

Friedrich-Alexander-Universität Erlangen, Institute  
for Medical Physics, Erlangen, Germany  
e-mail: [bernhard.schmidt@siemens-healthineers.com](mailto:bernhard.schmidt@siemens-healthineers.com)

T. Flohr  
Siemens Healthcare GmbH, Computed Tomography,  
Forchheim, Germany

Eberhard-Karls-Universität Tübingen, Institute of  
Diagnostic and Interventional Radiology,  
Tübingen, Germany  
e-mail: [thomas.flohr@siemens-healthineers.com](mailto:thomas.flohr@siemens-healthineers.com)

In 2006 DE CT was reintroduced with the advent of dual source CT systems (Flohr et al. 2006) which enabled the acquisition of DE CT data without the significant limitations of the previous technology, rather a much wider clinical application spectrum. Since then, the utilization of DE CT has been growing steadily, prompted in part by the introduction of newer generations of dual source CT systems with further improved dual-energy performance. A few years later, the portfolio for DE data acquisition techniques was extended to non-dual source CT systems with the introduction of subsequent spiral scanning at different X-ray tube voltages (Twin Spiral; Siemens Healthineers, Germany). This—in a second development step—was further improved upon by adding just to the high voltage spiral portion of the Twin Spiral acquisition an additional pre-filtration, already being well established for dual source CT systems. Hereby a dual-energy separation comparable to second and third generation of dual source CT was accomplished. To further substantially reduce the time delay between the high and low voltage data acquisition, a few years later TwinBeam (Siemens Healthineers, Germany) was introduced to single source CT systems. In this system a split filter is added to the X-ray tube collimator box, allowing examinations even in case of high contrast dynamics as in a contrast-enhanced scan in the arterial phase.

From a clinical perspective, DE CT imaging proves far more valuable than standard CT scans because, unlike them, it provides functional information on top of the mere anatomical visualization (Schneider et al. 2014). Kidney stones can be differentiated (Primak et al. 2007; Scheffel et al. 2007; Stolzmann et al. 2010), the differential diagnosis of gout is possible (Mallinson et al. 2016), and lesions can be characterized by quantifying their iodine uptake (Graser et al. 2010). In oncology, structures more responsive to treatment may potentially be identified early during treatment by reduced iodine uptake rather than by mere lesion size measurements (Apfaltrer et al. 2012; Uhrig et al. 2013; Agrawal et al. 2014; Knobloch et al. 2014). Perfusion defects in the lung parenchyma in patients with pulmonary embolism are visible in DE scans (Pontana et al.

2008; Remy-Jardin et al. 2014; Apfaltrer et al. 2014), as well as post-traumatic bone bruises or bone-marrow infiltration of the spine in patients with multiple myeloma (Pache et al. 2010; Thomas et al. 2015). DE CT has been applied in the characterization of perfusion defects in the myocardium (Ruzsics et al. 2009; Vliegenthart et al. 2012), as well as the iron uptake of the liver in patients with liver iron overload (Luo et al. 2015; Werner et al. 2019). Maps of effective atomic numbers obtained with DE CT may be used to improve radiation treatment planning, particularly in proton therapy. The applications listed above are an incomplete list of clinically relevant DE applications which are available on Siemens CT machines, and are either already being applied clinically or currently evaluated.

Besides dedicated clinical DE applications like the ones mentioned above, acquired data also can be used for calculation of virtual mono-energetic images. Similar to raw data-based approaches back in 1986 (Kalender et al. 1986), high- and low-energy images can be used for decomposition into materials differing in photoelectric and Compton characteristics, such as water and iodine (Yu et al. 2012). The concentrations of both materials in each image pixel are calculated by means of an image-based material decomposition algorithm that requires calibration measurements for the attenuation of iodine in phantoms of different diameter for the different X-ray spectra. The concentrations are subsequently multiplied with predicted CT numbers per concentration at the desired pseudo mono-chromatic energy (derived from NIST tables) and summed up to form the final mono-energetic images. Pseudo mono-energetic images derived from image-based material decomposition have similar applications as raw data-based images. Metal artifacts are reduced at higher energies/keV (Mangold et al. 2014), the contrast of iodine and bone increases at lower energies. Like in raw data-based techniques, image noise is amplified at energy levels far away from the mean energy of the mixed images ( $\sim 70$  keV). To avoid this undesirable increase in noise, which not only limits the ultimate clinical benefit of mono-energetic images but also limits the gains from

improved iodine contrast-to-noise ratio at lower keV, a novel algorithm for the computation of pseudo mono-energetic images was recently introduced (Mono+, Siemens Healthcare, Forchheim, Germany) that efficiently reduces image noise in pseudo mono-energetic images at low and high keV (Grant et al. 2014). Using this approach, images at the target keV and images at optimal keV from a noise perspective (typically, minimum image noise is obtained at approximately 70 keV) are computed. By means of a frequency-split technique, both the images at the target keV and the images with minimum image noise level are broken down into two sets of sub-images. The first set contains only lower spatial frequencies and thus most of the object information, the second one contains the remaining high spatial frequencies and subsequently mostly image noise. Finally, the lower spatial frequency stack at the target keV is combined with the high spatial frequency stack at optimal keV from a noise perspective to combine the benefits of both image stacks, see Fig. 1.

The Mono+ technique can be used to significantly increase the iodine CNR in CT angiographic studies by computing pseudo mono-energetic images at low keV (Albrecht et al. 2019). It has been shown (Grant et al. 2014) that it may be more efficient to perform DE scans and compute pseudo mono-energetic images at 40 keV using Mono+ to optimize iodine CNR

than to perform low kV-scans, which is today the recommended method to improve iodine CNR. The image-based Mono+ approach is available for all DE data from Siemens CT systems, and levels of the pseudo mono-energetic images can be selected between 40 keV and 190 keV in steps of 1 keV. Figure 2 shows a clinical example for illustration.

Although clinical DE applications and the possibility for improved image quality and better contrast-to-noise ratio are well perceived in the medical community, one of the remaining challenges of dual-energy imaging is workflow and workflow optimizations. In general, DE processing on Siemens CT systems is mainly based on the high and low voltage image stacks, which can be flexibly stored in PACS, or loaded and processed retrospectively by the various DE application classes provided in the Siemens syngo Dual-Energy application—irrespective of which scanner of the Siemens Healthineers CT scanner portfolio is used for data acquisition. In addition, automated dual-energy processing is offered to users who prefer PACS-focused reading over interactive processing and expert viewing in the syngo Dual-Energy application. User selected combinations of DE results are processed and transferred to the user-owned PACS fully automatically, thus being available whenever and wherever the user may need them, even for retrospective analysis. The most established mecha-

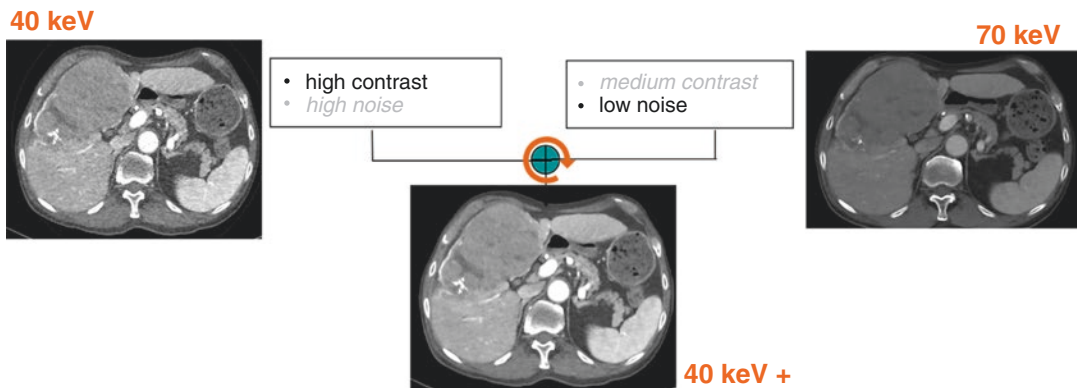


**Fig. 1** Schematic illustration of the concept used to calculate Mono+ images. In this example, the CNR of iodine versus soft tissue is enhanced. Images with high iodine contrast and high image noise (40 keV) are mixed with

images showing lower iodine contrast and lower noise (70 keV) to obtain improved CNR at low keVs (Grant et al. 2014)

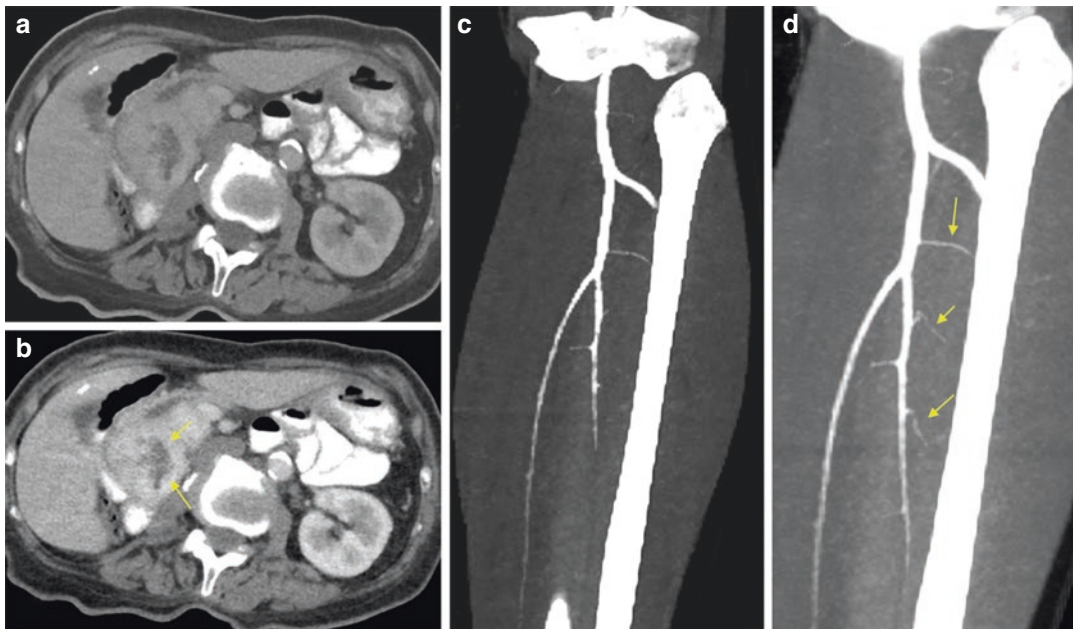


**Fig. 2** Left: DE images acquired on a third-generation DSCT scanner through the upper abdomen using the kV-combination 80 kV/150 kV with tin filter, and only 30 cc IV contrast media. Improved contrast and better lesion discernability in case of Mono+ at low keVs (b) compared to a mixed image, corresponding to a standard 120 kV

acquisition (a). Right: Pseudo mono-energetic image using the Mono+ technique at 50 keV (d) compared to 80 kV (c). Note the significantly increased iodine CNR of vascular structures with Mono+. (Courtesy of NYU Medical Center, Department of Radiology, New York, USA)

nisms for this workflow are “Rapid Results Technology” or “Recon&Go Inline Results.” Here the user has the ability to define at the scanner which processing steps should happen automatically, such as the generation of oblique Mono+ images or classified VRT images from a DE renal calculi application. Respective data are then processed automatically, and the results sent to the PACS system for further reading allowing for an efficient and integrated DE workflow (see Fig. 3).

One basic assumption for image-based material decomposition—used in the Siemens approach—is the validity of the thin absorber model. If we use water and iodine, for example, as the basis materials for image-based dual-energy evaluation, the maximum X-ray attenuation coefficient  $\mu_1(E)$  and the maximum thickness  $d_1$  of the iodine along any measured ray path are expected to be so small that it is valid to assume a linear contribution of the additional non-water-like attenuation  $\mu_1(E) \cdot d_1$  to the total attenuation.

It can be shown that the thin absorber model breaks down for iodine samples with more than 5000 HU cm in water based on 120 kV, which corresponds to the clinical situation of an object with 200 HU iodine enhancement and 25 cm thickness. In almost all clinically relevant situations, the thin absorber model remains valid. Exceptions are scan scenarios where extremely high iodine concentrations may be present, such as CT urographic scans.

In addition, the thin absorber model is based on the concept of an effective spectrum: the measured absorption with a polychromatic X-ray spectrum is assumed to be independent of the spatial distribution of the traversed materials along the beam. In practice, this means that neither the CT-value of water nor the CT-value of a small iodine sample depends on its position within the scanned object. The scanner must therefore be equipped with a bowtie filter of sufficient beam hardening and the approximately cylindrical patient cross-section has to be cen-

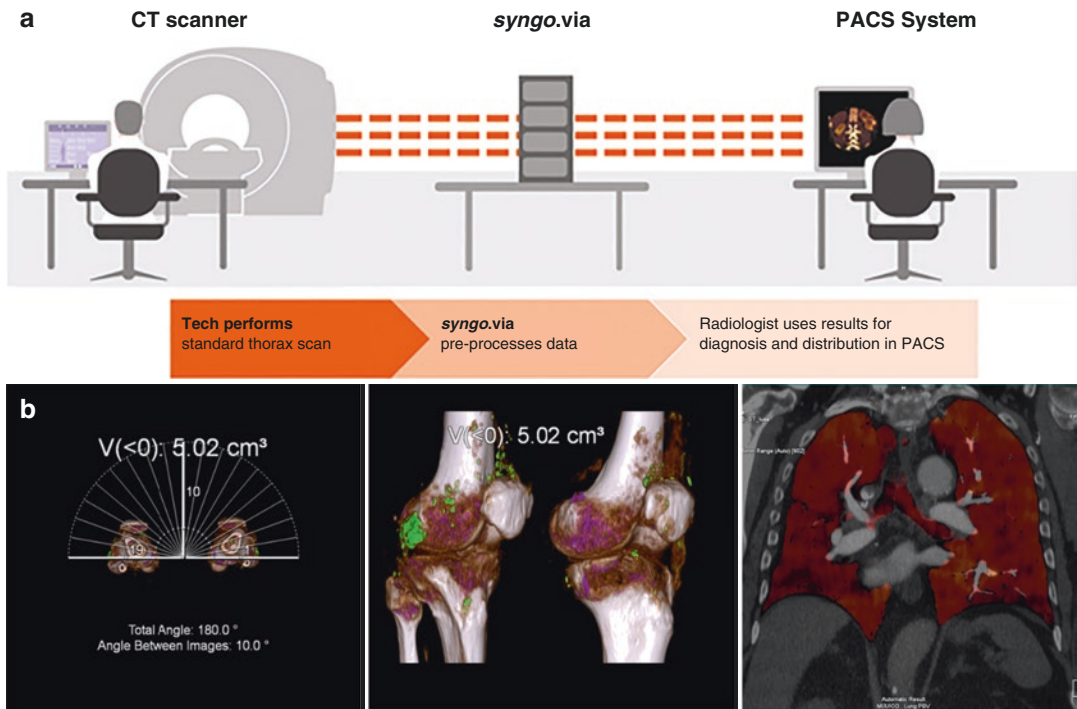


**Fig. 3** Optimized workflow on Siemens CT systems: Acquired DE image data are automatically labeled, processed by syngo via in the background and sent to PACS using Rapid Results Technology without any additional user interactions (**a**). Alternatively, on selected CT models a similar automatic advanced processing is possible directly at the scanner, where yet again results are processed self-operationally and sent directly to PACS for

further reading. Examples for respective results are shown in (**b**), where in addition to the visualization of DE results the gout volume is automatically calculated (in this example  $5.02 \text{ cm}^3$ ). Beside material and Mono+ images, anatomically oriented DE VRTs with classified results (left and middle) and fused images (right: overlay of mixed and iodine) can be generated

tered within the SFOV. In a real-world setting, electronics noise, scanner calibration, stability of emitted spectra, cone beam effects, and scattered radiation can have a larger impact on the obtained results than the analysis method.

As stated in the beginning of this article, Siemens is processing—irrespectively of the CT system type used for acquisition—based on low and high voltage image stacks. This makes storing of images, transferring and retrospective application of various DE classes easy. On the data acquisition side Siemens offers various solutions—depending on the technical capabilities of the respective CT system. In the following paragraphs, the different concepts and technical realizations are introduced and discussed.

## 2 Dual Source-Based Dual-Energy

A dual source CT is a CT system with two measurements systems, such as two X-ray tubes and the corresponding detectors. Both measurement systems acquire scan data simultaneously at the same anatomical level of the patient (same z-position). In 2006, the first dual source CT (DSCT) was commercially introduced by Siemens, the SOMATOM Definition (Siemens Healthcare GmbH, Forchheim, Germany), see Fig. 4.

The two acquisition systems A and B are mounted onto the rotating gantry at an angular offset of  $90^\circ$  for the first-generation DSCT (Flohr



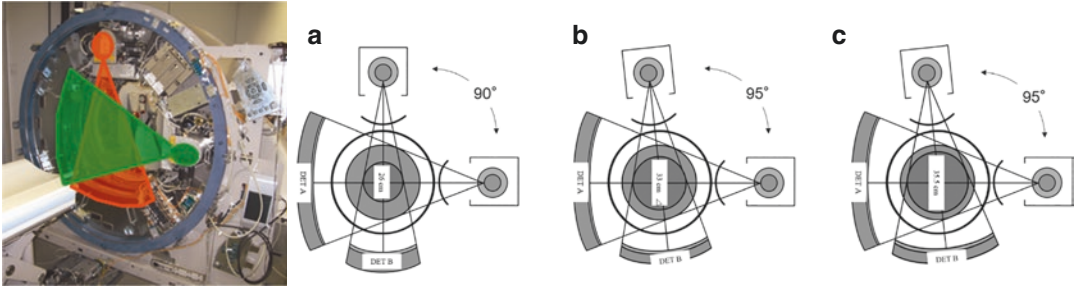


**Fig. 4** DSCT with two independent measurement systems. Left: Open gantry of a dual source CT system—red and green fans indicate the beams of the two X-ray tubes. (a) First generation: The system angle between both mea-

surement systems is  $90^\circ$ . (b) Second generation: To increase the SFOV of detector B, a larger system angle of  $95^\circ$  was chosen. With the third-generation DSCT (c), the SFOV of detector B was further increased to 35.5 cm

et al. 2006), and at an angular offset of  $95^\circ$  for the second- and third-generation DSCT. Detector A covers the full SFOV of 50 cm diameter, while detector B is restricted to a smaller FOV of 26 cm (first generation), 33 cm (second generation), or 35.6 cm (third generation) as a consequence of space limitations on the gantry. The shortest gantry rotation times are 0.33 s (first generation), 0.28 s (second generation), and 0.25 s (third generation). DSCT systems provide significantly improved temporal resolution for cardio-thoracic imaging. The shortest data acquisition time for an image corresponds to a quarter of the gantry rotation time (Flohr et al. 2006). Meanwhile, several clinical studies have demonstrated the potential of DSCT to accurately assess coronary artery stenosis in patients with high and irregular heart rates (Achenbach et al. 2006, Johnson et al. 2006, Scheffel et al. 2006, Matt et al. 2007, Leber et al. 2007, Ropers et al. 2007).

Moreover, with a DSCT system, dual-energy data can be acquired by simultaneously operating both X-ray tubes at different kV settings, e.g., 80 kV and 140 kV (Flohr et al. 2006; Johnson et al. 2007). Scan parameters (e.g., tube current and potential) can be adjusted individually for both measurement systems, resulting in a balanced radiation dose distribution between the low- and the high-energy scans. A wide range of routine scan protocols is available, with no

restrictions in the choice of scan parameters such as gantry rotation time. Use of anatomical tube current modulation allows for adaptation of the radiation dose to the patient's anatomy. Mixed images (a weighted average of low- and high-energy images) and Mono+ are routinely available, allowing dual-energy CT scans to be performed in routine clinical practice similar to conventional imaging protocols, with dual-energy information available when needed. It should be noted that dual-energy imaging and the ability for Mono+ as well as iodine quantification being helpful, e.g., for the assessment of the perfusion of the myocardium is also possible for gated cardiac scans on dual source systems. An example is shown in Fig. 5.

Spectral separation, a key measure for DE performance, can be improved by introducing additional pre-filtration into the high kV beam, e.g., by means of a filter that can be moved into the beam when needed and moved out for standard applications. The quality of DE CT examinations generally relies on the separation of the energy spectra. High spectral overlap and bad energy separation result in increased image noise in the base-material decomposition which in turn requires compensation by increased radiation dose. The second-generation DSCT makes use of an additional tin filter (Sn) with a thickness of 0.4 mm to shift the mean energy of the 140 kV

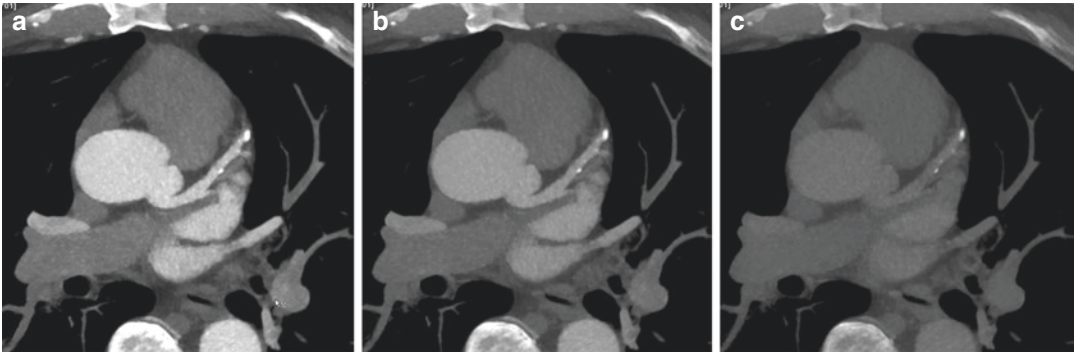


**Fig. 5** ECG-triggered “step-and-shoot” DE cardiac CT acquisition using a third-generation DSCT at 90 kV/150 Sn kV, rotation time 0.25 s: Based on the acquired data, images with 66 ms temporal resolution can be reconstructed. In addition, since data from A and B are

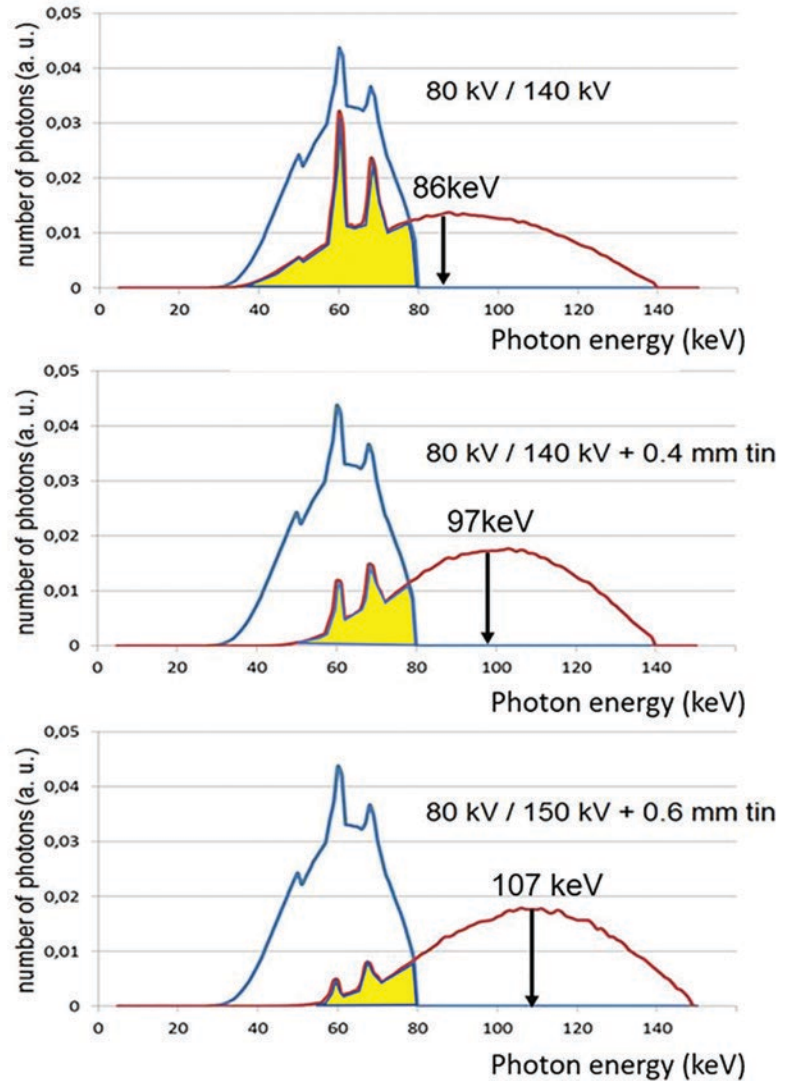
acquired simultaneously, DE information can be used to optimize iodine contrast in coronary vessels based on Mono+ imaging: 55 keV (a), 70 keV (b), and 110 keV (c). Courtesy of Medical University of South Carolina, Charleston, USA

spectrum from 86 keV to 97 keV (after 20 cm water), see Fig. 6. The mean energy of the 80 kV spectrum is 60 keV. The third-generation DSCT provides 150 kV X-ray tube voltage with more aggressive tin pre-filtration (0.6 mm), shifting the mean energy of the 150 kV spectrum to 107 keV, see also Fig. 6. The tin filter improves spectral separation between the low- and high-energy spectra, narrows the high kV spectrum (which results in better dose efficiency and less beam hardening artifacts), and reduces the influence of cross-scattering. A relevant parameter to quantify the performance of a DE CT acquisition technique with regard to energy separation and material differentiation capability is the Dual-Energy (DE) ratio. The DE ratio of a material is defined as its CT number (in HU) at low kV divided by its CT number (in HU) at high kV (Krauss et al. 2015). Water has a DE ratio of 1, meaning its CT number does not change in CT scans at different kV settings. The DE ratio for iodine, a commonly used base material for material decomposition in contrast-enhanced CT scans, increases from 1.9 to 2 at the standard 80 kV/140 kV X-ray tube voltage combination to about 3.4 for 80 kV/150 kV and 0.6 mm tin pre-filtration (measured in a 20 cm water phantom, Krauss et al.

2015). The larger DE ratio results in better conditioned equations for base-material differentiation into, for example, water and iodine as base materials, and leads to less image noise in the material-specific images. Consequently, this enables DE data acquisition at the radiation dose of typical medical CT examinations, without additional dose penalty, see, e.g., (Schenzle et al. 2010; Bauer et al. 2011; Henzler et al. 2012).

As a downside, DE evaluation with dual source CT is restricted to the smaller central SFOV of detector B. Raw data-based dual-energy algorithms cannot be realized because high-energy and low-energy projections are not simultaneously acquired at the same z-position. Dual-energy algorithms are therefore image-based. Another challenge of dual source DE CT is cross-scattered radiation, i.e., scattered radiation originating from tube A and detected by detector B, and vice versa, which has to be carefully corrected for to avoid distortions of CT numbers by cupping or streaking artifacts. This can be done either by measurement of cross-scattered radiation or by model-based approaches (Petersilka et al. 2010). Figure 7 shows a clinical example of a DE CT scan acquired with a third-generation DSCT system.

**Fig. 6** Typical 80 kV and 140 kV spectra (after 20 cm water), normalized to equal areas under the curves (top). 80 kV spectrum and 140 kV spectrum with additional 0.4 mm tin pre-filtration (center), and 80 kV spectrum and 150 kV spectrum with additional 0.6 mm tin pre-filtration (bottom). Note the shift of the mean energy of the high-energy spectrum to higher values (arrow) and the reduced spectral overlap. The yellow marked areas indicate the portion of the spectra that measured redundant information



### 3 Twin Spiral Dual-Energy

For non-dual source CT systems, the most straightforward approach for acquiring dual-energy CT data are two subsequent CT scans of the same anatomical structure, one with low X-ray tube voltage (80 kV), the other with high X-ray tube voltage (140 kV). The spectral separation achieved with this approach is reasonably effective. DE CT is feasible with standard CT systems

with a 50 cm diameter full scan field of view (SFOV). However, the disadvantage is that the time delay between the two scans presents a challenge for the evaluation of fast moving organs. Furthermore, examinations with administration of contrast agent are challenging, at least in early arterial phases when the contrast density changes rapidly between the two scans. The resulting CT-number changes will be misinterpreted by DE material decomposition techniques.



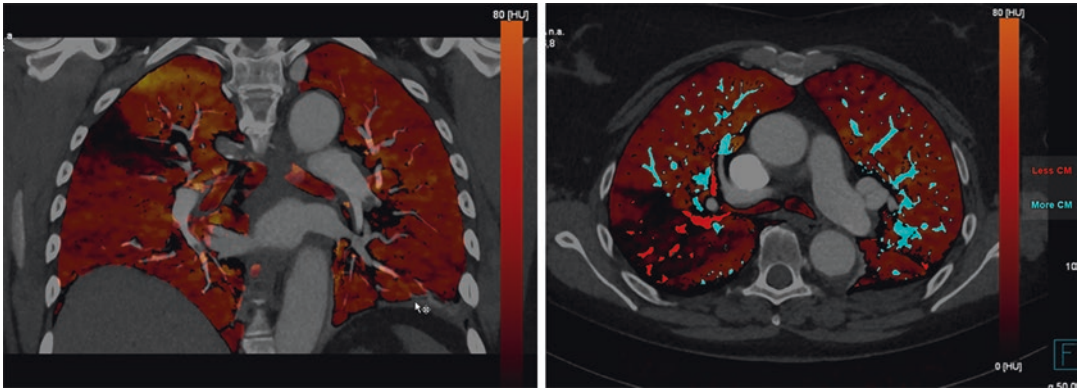


**Fig. 7** Contrast-enhanced DE CT scan of a patient with acute pulmonary embolism acquired with a third-generation DSCT scanner at 90 kV/150 kV with 0.6 mm tin pre-filtration. Left: Mixed image overlaid by the quantitative perfusion information of the lung parenchyma, showing a v-like perfusion defect caused by an

occluding clot. Right: In addition to parenchymal information, DE-based color-coding of the vessel lumen. Non-iodinated vessels—matching with the perfusion defect—are highlighted in red. Courtesy of University Hospital of Frankfurt, Germany

A technical realization was first introduced with the SOMATOM Definition AS, SOMATOM Edge (Siemens Healthcare GmbH, Forchheim, Germany), where the DE acquisition relies on two automatically, workflow-wise completely coupled spiral (helical) scans of the same body region, the first performed at 80 kV and the second at 140 kV. The approach to go for volumetric acquisitions instead of a single axial scan is advantageous since mismatch due to motion can be corrected by a respective volumetric registration approach. As in standard CT examinations, radiation dose to the patient can be optimized by anatomical tube current modulation (Marin et al. 2014), and iterative reconstruction can be applied. Because of the small time delay between the two spiral scans, the use of this technique is indicated for non-dynamic examinations that do not require the administration of contrast agent, such as characterization of kidney stones, or the examination of tophaceous lesions in patients with gout, or for the calculation of pseudo mono-energetic images to reduce metal artifacts at a metal-specific high energy.

With the introduction of the SOMATOM X. Cite in 2019 and the SOMATOM X.ceed 2021, Siemens introduced tin filtration that had already been well established in Dual Source CT systems to Twin Spiral scanning, allowing for a substan-

tial improvement of spectral separation and better DE performance (see Fig. 8). A clinical example is shown in Fig. 9, where a voltage combination of 80 kV and 150 Sn kV had been used.

#### 4 TwinBeam Dual-Energy

Recently, a new method was introduced to acquire DE CT data with a single source CT system without kV-switching, but with better temporal registration than by performing two separate consecutive axial or spiral scans of the examination volume of interest. Two different pre-filters in the tube collimator housing are used to split the X-ray beam in the scan direction, called “TwinBeam” (e.g., on SOMATOM Definition Edge, Siemens Healthcare GmbH, Forchheim, Germany), see Fig. 10.

The X-ray tube is operated at 120 kV tube voltage. One half of the multi-slice detector in the scan direction is illuminated by an X-ray beam pre-filtered with 0.6 mm tin; compared to the standard 120 kV spectrum, the mean energy of this pre-filtered spectrum is increased, see Fig. 10, right. The other half of the detector in the scan direction is pre-filtered with a thin gold filter; as a consequence of the K-edge of gold at 80.7 keV, the mean energy of this spectrum is decreased, see Fig. 10, right. The total attenuation of the pre-filters is adjusted to bal-

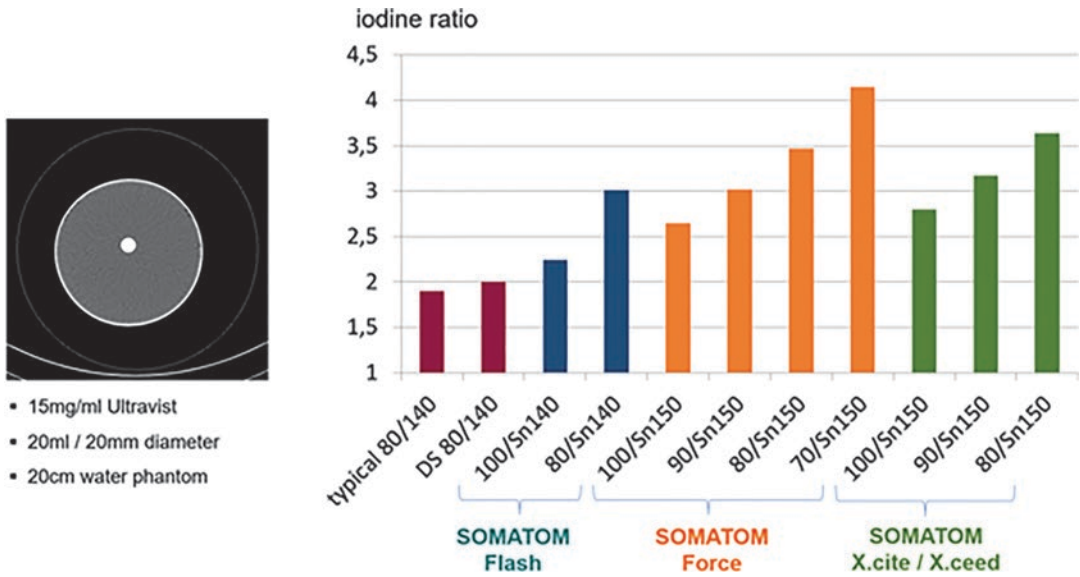


**Fig. 8** DE performance can be measured quantitatively in terms of iodine ratio (HU at low energy divided by HU at high energy): For the high kV beam, additional tin filtration was introduced for dual systems to improve DE

performance. Additional tin filtration of 0.7 mm introduced with the SOMATOM X.cite and X.ceed, increases dual-energy separation for Twin Spiral into the range of second- and third-generation dual source CTs

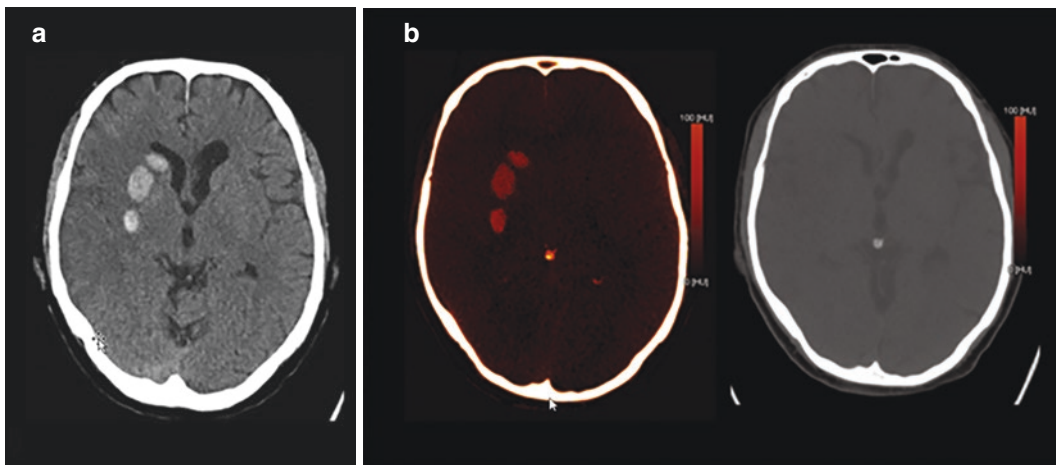


**Fig. 9** Clinical example for dual-energy imaging technique relying on two consecutive spiral scans (Twin Spiral) at 80 kV and 150 Sn kV on SOMATOM X.cite. Post-thrombectomy follow-up CT: Hyperattenuating intraparenchymal area visible in the conventional mixed

image (a). Iodine overlay image (b) derived from spectral information reveals that area of hyper-attenuation corresponds to an area of diffused contrast material extravasation. Virtual non-contrast image excludes active bleeding. Courtesy of University Hospital Zurich, Switzerland

ance the radiation dose of the low-energy and the high-energy beam. The CT system is operated in a spiral (helical) scan mode at fast gantry rotation speed (0.28 s) with a maximum spiral pitch of 0.5 (referring to the full z-width of the detector). Moreover, recently introduced CT systems equipped with a split filter, the SOMATOM go.Top,

X.cite and X.ceed, even allow for adaptation of tube voltage. Depending on the clinical need and the size of the patient (attention information is derived from the topogram), either 120 kV or 140 kV is selected for the use with the split filter. The possibility for a higher voltage is of advantage for two reasons: First, spectral separation is increased. Secondly,

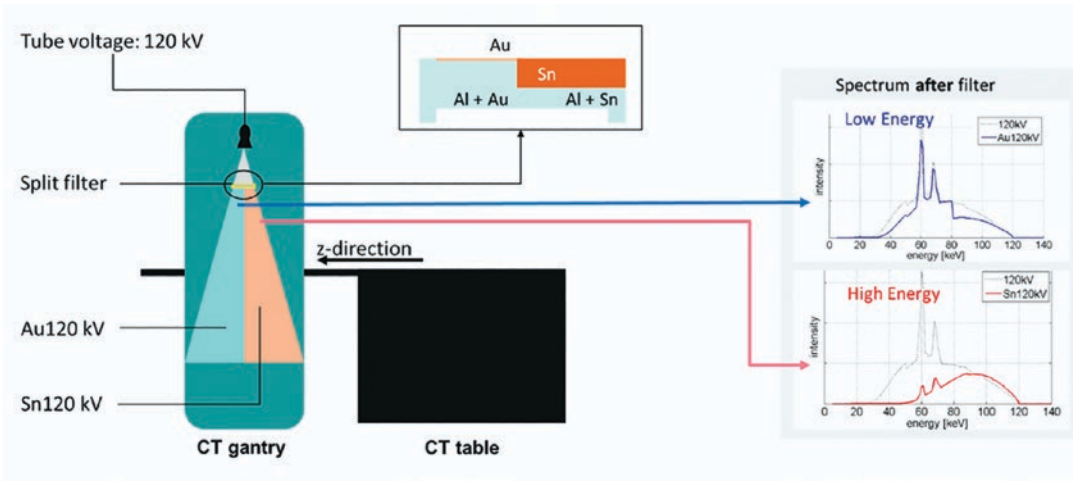


**Fig. 10** Left: Principle of a DE acquisition technique that uses a split filter, called “TwinBeam” (Siemens Healthcare GmbH, Forchheim, Germany), in the tube collimator housing to split the X-ray beam in the scan direction.

Right: The standard 120 kV spectrum is split into a low-energy spectrum after filtering with gold (Au, top), and a high-energy spectrum after filtering with tin (Sn, bottom)

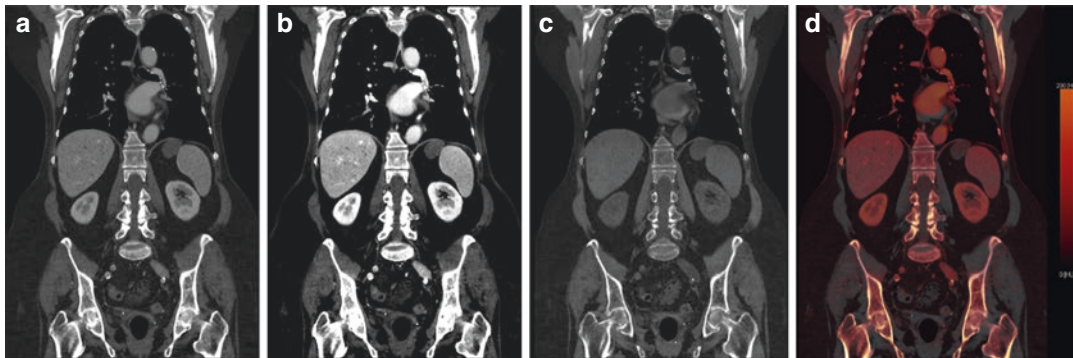


**Fig. 11** Contrast-enhanced thorax-abdominal CT examination on a SOMATOM X.cite using Twin Spiral technique. From the acquired DE data, Mono+ images can be generated to increase iodine contrast. At lower energies of 45 keV (b), delineation of anatomical structures and con-

spicuity of lesions is improved compared to 70 keV images (a). In addition, virtual non-contrast images (c) and iodine—as overlay—images (d) can be extracted. The latter in particular allows for quantitative analysis of iodine distribution. Courtesy of Erlangen University, Germany

140 kV allows for a higher tube output and enables scanning of larger patients. Then, for the reconstruction of the TwinBeam data, each half of the detector acquires a complete spiral data set because of the lower spiral pitch, allowing for low- and high-energy images to be reconstructed at any z-position as an input into Mono+ and/ or image-based material decomposition techniques.

This technology provides DE data in the full SFOV of 50 cm diameter. The radiation dose to the patient can be optimized by means of anatomical tube current modulation or risk organ-dependent tube current modulation, in addition to iterative

reconstruction techniques. The data sets are temporally registered, enabling DE CT scans with contrast agent even in the arterial phase. The downside of this approach is that spectral separation is worse than with approaches using two different kV-settings of the X-ray tube. Furthermore, a powerful X-ray tube is required because the pre-filtration absorbs a considerable portion of the X-ray flux, in turn limiting the use of this technique to non-obese patients. Because of the maximum spiral pitch of 0.5, maximum volume coverage speed is limited. Figure 11 shows a clinical example acquired with the split filter technique.

## 5 Conclusions

Since 2006, with the introduction of DE on Dual Source CT systems, DE imaging has experienced a renaissance. Its clinical application spectrum is growing, and different technical solutions for data acquisition are available. With ongoing technological progress, such as improved spectral separation by means of dedicated pre-filtration of the high-energy beam, successful DE applications have been demonstrated without increased radiation dose to the patient compared to standard single energy CT scans. The dual source dual-energy CT solution provides technical and clinical advantages, such as flexible selection of the kVs of the low-energy beam allows for optimized scanning, adapted to clinical needs. The wide detector coverage combined with the high rotation time allows scanning of even challenging patients, for example those short of breath. Twin Spiral and TwinBeam are alternatives available for single source CTs. Despite the different technical realizations, the same image-based automatic processing techniques and processing applications are applied, allowing the use of DE in a routine clinical workflow.

### Compliance with Ethical Standards

**Disclosure of Interests** Bernhard Schmidt and Thomas Flohr are employees of Siemens Healthineers.

## References

- Achenbach S, Ropers D, Kuettner A, Flohr T, Ohnesorge B, Bruder H, Theessen H, Karakaya M, Daniel WG, Bautz W, Kalender WA, Anders K (2006) Contrast-enhanced coronary artery visualization by dual-source computed tomography – initial experience. *Eur J Radiol* 57(3):331–335
- Agarwal MD, Pinho DF, Kulkarni NM, Hahn PF, Guimaraes AR, Sahani DV (2014) Oncologic applications of dual-energy CT in the abdomen. *Radiographics* 34(3):589–612
- Albrecht MH, Vogl TJ, Martin SS, Nance JW, Duguay TM, Wichmann JL, De Cecco CN, Varga-Szemes A, van Assen M, Tesche C, Schoepf UJ (2019) Review of clinical applications for virtual monoenergetic dual-energy CT. *Radiology* 293(2):260–271
- Apfaltrer P, Meyer M, Meier C, Henzler T, Barraza JM Jr, Dinter DJ, Hohenberger P, Schoepf UJ, Schoenberg SO, Fink C (2012) Contrast-enhanced dual-energy CT of gastrointestinal stromal tumors: is iodine-related attenuation a potential indicator of tumor response? *Invest Radiol* 47(1):65–70
- Apfaltrer P, Sudarski S, Schneider D et al (2014) Value of monoenergetic low-kV dual energy CT datasets for improved image quality of CT pulmonary angiography. *Eur J Radiol* 83:322–328
- Bauer RW, Kramer S, Renker M et al (2011) Dose and image quality at CT pulmonary angiography: comparison of first and second generation dual energy CT and 64-slice CT. *Eur Radiol* 21:2139–2147
- Flohr TG, McCollough CH, Bruder H, Petersilka M, Gruber K, Süß C, Grasruck M, Stierstorfer K, Krauss B, Raupach R, Primak AN, Küttner A, Achenbach S, Becker C, Kopp A, Ohnesorge BM (2006) First performance evaluation of a dual-source CT (DSCT) system. *Eur Radiol* 16(2):256–268
- Genant HK, Boyd D (1977) Quantitative bone mineral analysis using dual energy computed tomography. *Invest Radiol* 12(6):545–551
- Grant KL, Flohr TG, Krauss B, Sedlmair M, Thomas C, Schmidt B (2014) Assessment of an advanced image-based technique to calculate virtual monoenergetic computed tomographic images from a dual-energy examination to improve contrast-to-noise ratio in examinations using iodinated contrast media. *Invest Radiol* 49(9):586–592
- Graser A, Becker CR, Staehler M et al (2010) Single-phase dual-energy CT allows for characterization of renal masses as benign or malignant. *Invest Radiol* 45(7):399–405
- Henzler T, Fink C, Schoenberg SO, Schoepf UJ (2012) Dual energy CT: radiation dose aspects. *Am J Roentgenol* 199:S16–S25
- Johnson TRC, Nikolaou K, Wintersperger BJ, Leber AW, von Ziegler F, Rist C, Buhmann S, Knez A, Reiser MF, Becker CR (2006) Dual source cardiac CT imaging: initial experience. *Eur Radiol* 16:1409–1415
- Johnson TRC, Krauß B, Sedlmair M, Grasruck M, Bruder H, Morhard D, Fink C, Weckbach S, Lenhard M, Schmidt B, Flohr T, Reiser MF, Becker CR (2007) Material differentiation by dual energy CT: initial experience. *Eur Radiol* 17(6):1510–1517
- Kalender W (1987) Vertebral bone mineral analysis. *Radiology* 164:419–423
- Kalender WA, Perman WH, Vetter JR, Klotz E (1986) Evaluation of a prototype dual-energy computed tomographic apparatus. I. Phantom studies. *Med Phys* 13(3):334–339
- Knobloch G, Jost G, Huppertz A, Hamm B, Pietsch H (2014) Dual-energy computed tomography for the assessment of early treatment effects of regorafenib in a preclinical tumor model: comparison with dynamic contrast-enhanced CT and conventional contrast-enhanced single-energy CT. *Eur Radiol* 24(8):1896–1905



- Krauss B, Grant KL, Schmidt BT, Flohr TG (2015) The importance of spectral separation: an assessment of dual-energy spectral separation for quantitative ability and dose efficiency. *Invest Radiol* 50(2):114–118
- Laval-Jeantet AM, Roger B, Bouysee S, Bergot C, Mazess RB (1986) *Radiology* 159(2):463–6. <https://doi.org/10.1148/radiology.159.2.3961178>.
- Leber AW, Johnson T, Becker A, von Ziegler F, Tittus J, Nikolaou K, Reiser M, Steinbeck G, Becker CR, Knez A (2007) Diagnostic accuracy of dual-source multislice CT-coronary angiography in patients with an intermediate pretest likelihood for coronary artery disease. *Eur Heart J* 28(19):2354–2360
- Luo XF, Xie XQ, Cheng S, Yang Y, Yan J, Zhang H, Chai WM, Schmidt B, Yan FH (2015) Dual-energy CT for patients suspected of having liver iron overload: can virtual iron content imaging accurately quantify liver iron content? *Radiology* 277(1):95–103
- Mallinson PI, Coupal TM, McLaughlin PD, Nicolaou S, Munk PL, Ouellette HA (2016) Dual-energy CT for the musculoskeletal system. *Radiology* 281(3):690–707
- Mangold S, Gatidis S, Luz O, König B, Schabel C, Bongers MN, Flohr TG, Claussen CD, Thomas C (2014) Single-source dual-energy computed tomography: use of monoenergetic extrapolation for a reduction of metal artifacts. *Invest Radiol* 49(12):788–793
- Marin D, Boll DT, Mileto A, Nelson RC (2014) State of the art: dual-energy CT of the abdomen. *Radiology* 271(2):327–342
- Matt D, Scheffel H, Leschka S, Flohr TG, Marincek B, Kaufmann PA, Alkadhi H (2007) Dual-source CT coronary angiography: image quality, mean heart rate, and heart rate variability. *Am J Roentgenol* 189(3):567–573
- Pache G, Krauss B, Strohm P, Saueressig U, Blanke P, Bulla S, Schäfer O, Helwig P, Kotter E, Langer M, Baumann T (2010) Dual-energy CT virtual noncalcium technique: detecting posttraumatic bone marrow lesions – feasibility study. *Radiology* 256(2):617–624
- Petersilka M, Stierstorfer K, Bruder H, Flohr T (2010) Strategies for scatter correction in dual source CT. *Med Phys* 37:5971–5992
- Pontana F, Faivre JB, Remy-Jardin M et al (2008) Lung perfusion with dual-energy multidetector-row CT (MDCT): feasibility for the evaluation of acute pulmonary embolism in 117 consecutive patients. *Acad Radiol* 15(12):1494–1504
- Primak AN, Fletcher JG, Vrtiska TJ, Dzyubak OP, Lieske JC, Jackson ME, Williams JC Jr, McCollough CH (2007) Noninvasive differentiation of uric acid versus non-uric acid kidney stones using dual-energy CT. *Acad Radiol* 14(12):1441–1447
- Remy-Jardin M, Faivre JB, Pontana F, Molinari F, Tacelli N, Remy J (2014) Thoracic applications of dual energy. *Semin Respir Crit Care Med* 35(1):64–73
- Ropers U, Ropers D, Pflederer T, Anders K, Kuettner A, Stilianakis NI, Komatsu S, Kalender W, Bautz W, Daniel WG, Achenbach S (2007) Influence of heart rate on the diagnostic accuracy of dual-source computed tomography coronary angiography. *J Am Coll Cardiol* 50(25):2393–2398
- Ruzsics B, Schwarz F, Schoepf UJ et al (2009) Comparison of dual-energy computed tomography of the heart with single photon emission computed tomography for assessment of coronary artery stenosis and of the myocardial blood supply. *Am J Cardiol* 104(3):318–326
- Scheffel H, Alkadhi H, Plass A, Vachenaue R, Desbiolles L, Gaemperli O, Schepis T, Frauenfelder T, Schertler T, Husmann L, Grunenfelder J, Genoni M, Kaufmann PA, Marincek B, Leschka S (2006) Accuracy of dual-source CT coronary angiography: first experience in a high pre-test probability population without heart rate control. *Eur Radiol* 16(12):2739–2747
- Scheffel H, Stolzmann P, Frauenfelder T, Schertler T, Desbiolles L, Leschka S, Marincek B, Alkadhi H (2007) Dual-energy contrast-enhanced computed tomography for the detection of urinary stone disease. *Invest Radiol* 42(12):823–829
- Schenzle JC, Sommer WH, Neumaier K et al (2010) Dual energy CT of the chest: how about the dose? *Invest Radiol* 45:347–353
- Schneider D, Apfaltrer P, Sudarski S et al (2014) Optimization of kiloelectron volt settings in cerebral and cervical dual-energy CT angiography determined with virtual monoenergetic imaging. *Acad Radiol* 21:431–436
- Stolzmann P et al (2010) In vivo identification of uric acid stones with dual-energy CT: diagnostic performance evaluation in patients. *Abdom Imaging* 35(5):629–635
- Thomas C, Schabel C, Krauss B, Weisel K, Bongers M, Claussen CD, Horger M (2015) Dual-energy CT: virtual calcium subtraction for assessment of bone marrow involvement of the spine in multiple myeloma. *Am J Roentgenol* 204(3):W324–W331
- Uhrig M, Sedlmair M, Schlemmer HP, Hassel JC, Ganten M (2013) Monitoring targeted therapy using dual-energy CT: semi-automatic RECIST plus supplementary functional information by quantifying iodine uptake of melanoma metastases. *Cancer Imaging* 13(3):306–313
- Vetter JR, Perman WH, Kalender WA, Mazess RB, Holden JE (1986) Evaluation of a prototype dual-energy computed tomographic apparatus. II. Determination of vertebral bone mineral content. *Med Phys* 13(3):340–3. <https://doi.org/10.1118/1.595951>.
- Vliegenthart R, Pilgrim GJ, Ebersberger U, Rowe GW, Oudkerk M, Schoepf U (2012) Dual-energy CT of the heart. *Am J Roentgenol* 199:S54–S63
- Werner A, Krauss B, Haberland U, Bongers M, Starke U, Bakchoul T, Enkel S, Nikolaou K, Horger M (2019) Dual-energy CT for liver iron quantification in patients with haematological disorders. *Eur Radiol* 29(6):2868–2877
- Yu L, Leng S, McCollough C et al (2012) Dual-energy CT-based monochromatic imaging. *Am J Roentgenol* 199(5 Suppl):S9–S15